Vol 15 No 11, November 2006
1009-1963/2006/15(11)/2661-08

Chinese Physics

© 2006 Chin. Phys. Soc.
and IOP Publishing Ltd

Study of the double rectangular waveguide grating slow-wave structure*

Lu Zhi-Gang(路志刚)†, Gong Yu-Bin(宫玉彬),
Wei Yan-Yu(魏彦玉), and Wang Wen-Xiang(王文祥)

School of Physical Electronics, University of Electronic Science and Technology of China, Chengdu 610054, *China*

(Received 20 February 2006; revised manuscript received 6 June 2006)

A slow-wave structure (SWS) with two opposite gratings inside a rectangular waveguide is presented and analysed. As an all-metal slow-wave circuit, this structure is especially suited for use in millimetre-wave travelling wave tubes (TWTs) due to its advantages of large size, high manufacturing precision and good heat dissipation. The first part of this paper concerns the wave properties of this structure in vacuum. The influence of the geometrical dimensions on dispersion characteristics and coupling impedance is investigated. The theoretical results show that this structure has a very strong dispersion and the coupling impedance for the fundamental wave is several tens of ohms, but the coupling impedance for –1 space harmonic wave is much lower than that for the fundamental wave, so the risk of backward wave oscillation is reduced. Besides these, the CST microwave studio is also used to simulate the dispersion property of the SWS. The simulation results from CST and the theoretical results agree well with each other, which supports the theory. In the second part, a small-signal analysis of a double rectangular waveguide grating TWT is presented. The typical small-signal gain per period is about 0.45 dB, and the 3-dB small-signal gain bandwidth is only 4%.

Keywords: TWT, rectangular waveguide grating, dispersion, small signal gain

PACC: 5270G, 4110H

1. Introduction

Recently, owing to a demand for advanced radar and communications, the high-frequency and high-power sources have been developed with frequencies between 100 and 300 GHz and peak powers as high as several hundreds of kilowatts, and a bandwidth of up to 10%. Since the investigation of the interaction mechanisms of different slow-wave structures (SWSs), the rectangular waveguide grating SWS,[1−10] which is used in numerous microwave oscillator and amplifier experiments, has aroused much interest of all due to its unique features: the scalability to smaller dimensions and shorter wavelengths, high precision of manufacturing and assembling, super-thermal conductivity and low loss, which make it worth being investigated, especially at millimetre-wave frequency-band. In our previous work, a single rectangular waveguide grating was analysed.[11] This paper presents an analysis of a slow-wave structure, called the double rectangular waveguide gratings, composed of two opposite gratings in a rectangular waveguide as illustrated in Fig.1.

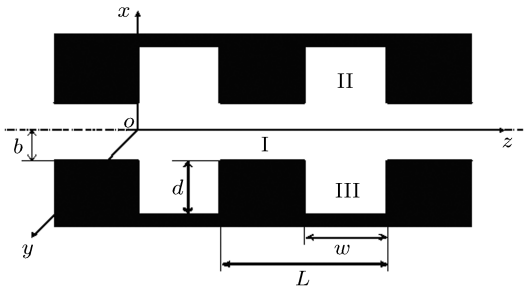


Fig.1. Configuration of the double rectangular waveguide grating circuit.

2. Wave properties in a double rectangular waveguide grating SWS

First, we investigate the wave properties including the dispersion relation and the interaction impedance of the structure in vacuum. Figure 1 is the sectional view through the xoz plane of the double rectangular waveguide grating slow-wave circuit model. An electromagnetic wave propagates along the surface of the gratings, and slows down in the z-direction. When

*Project supported by the State Key Program of National Natural Science of China (Grant No 60532010).
†E-mail: lzhgchnn@uestc.edu.cn

the phase velocity of the wave is synchronous with the beam, the energy transfers from the beam to the wave, thus the wave is amplified.

2.1. The field distribution

As shown in Fig.1, the structure is divided into three regions: interaction region I, groove region II and groove region III. The two gratings are symmetrical with respect to the yoz plane. L denotes the period of the gratings, w is the length of the slot openings, d is the depth of the slots, and $2b$ represents the spacing between the gratings. The width of waveguide is expressed by a. In the following analysis, the time-dependent $\exp(\mathrm{j}\,\omega t)$ is assumed (and suppressed) for all field quantities.

The slow-wave mode[4,5] supported by this structure is transversely electric with respect to the y-direction, i.e. TE_y under the assumption of $E_y = 0$. Both slow and fast waves may be excited due to the closeness of the circuit. Each of these waves consists of an infinite sum of space harmonics on account of the periodicity of the structure. Here, only the slow-wave mode is considered. Using Floquet's theorem and the Cartesian coordinates (x, y, z), the fields in region I can be written as

$$
\begin{aligned}
H_y^{\mathrm{I}} &= \sum_{n=-\infty}^{+\infty} [A_n^{\mathrm{I}} \sinh(v_x^{\mathrm{I}} x) + B_n^{\mathrm{I}} \cosh(v_x^{\mathrm{I}} x)] \sin(k_y^{\mathrm{I}} y) \mathrm{e}^{-\mathrm{j}\beta_n^{\mathrm{I}} z}, \\
E_x^{\mathrm{I}} &= \sum_{n=-\infty}^{+\infty} \frac{\omega\mu_0\beta_n^{\mathrm{I}}}{(h^{\mathrm{I}})^2} [A_n^{\mathrm{I}} \sinh(v_x^{\mathrm{I}} x) + B_n^{\mathrm{I}} \cosh(v_x^{\mathrm{I}} x)] \sin(k_y^{\mathrm{I}} y) \mathrm{e}^{-\mathrm{j}\beta_n^{\mathrm{I}} z}, \\
E_z^{\mathrm{I}} &= \sum_{n=-\infty}^{+\infty} -\frac{\mathrm{j}\omega\mu_0 v_x^{\mathrm{I}}}{(h^{\mathrm{I}})^2} [A_n^{\mathrm{I}} \cosh(v_x^{\mathrm{I}} x) + B_n^{\mathrm{I}} \sinh(v_x^{\mathrm{I}} x)] \sin(k_y^{\mathrm{I}} y) \mathrm{e}^{-\mathrm{j}\beta_n^{\mathrm{I}} z}, \\
H_x^{\mathrm{I}} &= \sum_{n=-\infty}^{+\infty} \frac{k_y^{\mathrm{I}}}{(h^{\mathrm{I}})^2} [A_n^{\mathrm{I}} \cosh(v_x^{\mathrm{I}} x) + B_n^{\mathrm{I}} \sinh(v_x^{\mathrm{I}} x)] \cos(k_y^{\mathrm{I}} y) \mathrm{e}^{-\mathrm{j}\beta_n^{\mathrm{I}} z}, \\
H_z^{\mathrm{I}} &= \sum_{n=-\infty}^{+\infty} -\frac{\mathrm{j}\beta_n^{\mathrm{I}} k_y^{\mathrm{I}}}{(h^{\mathrm{I}})^2} [A_n^{\mathrm{I}} \sinh(v_x^{\mathrm{I}} x) + B_n^{\mathrm{I}} \cosh(v_x^{\mathrm{I}} x)] \cos(k_y^{\mathrm{I}} y) \mathrm{e}^{-\mathrm{j}\beta_n^{\mathrm{I}} z},
\end{aligned} \tag{1}
$$

where A_n^{I} and B_n^{I} are the amplitude factors, μ_0 is the permeability, v_x^{I}, k_y^{I} and β_n^{I} are the wave numbers of the n space harmonic in the x-, y- and z-directions, respectively. $\beta_n^{\mathrm{I}} = \beta_0^{\mathrm{I}} + 2n\pi/L$, $k_y^{\mathrm{I}} = l\pi/a, (l = 1, 2, 3\cdots)$, $(h^{\mathrm{I}})^2 = k_0^2 - (k_y^{\mathrm{I}})^2$, $(v_x^{\mathrm{I}})^2 = (\beta_n^{\mathrm{I}})^2 - (h^{\mathrm{I}})^2$. $k_0 = \omega/c$ is the propagation constant in free space. ω is angular frequency and c is speed of light in vacuum.

In groove regions (II and III), we assume that the solution can be expressed by a Fourier series expansion as an infinite sum of standing eigen waves, which can be written as

$$
\begin{aligned}
H_y^i &= \sum_{m=0}^{+\infty} C_m^i F_m^i(x) \sin(k_y^i y) \cos(k_z^i z), \\
E_y^i &= \sum_{m=0}^{+\infty} -\frac{\mathrm{j}\omega\mu_0}{(h^i)^2} k_z^i C_m^i F_m^i(x) \sin(k_y^i y) \sin(k_z^i z), \\
E_z^i &= \sum_{m=0}^{+\infty} -\frac{\mathrm{j}\omega\mu_0}{(h^i)^2} C_m^i [F_m^i(x)]' \sin(k_y^i y) \cos(k_z^i z), \quad i = (\mathrm{II}, \mathrm{III}) \\
H_x^i &= \sum_{m=0}^{+\infty} \frac{k_y^i}{(h^i)^2} C_m^i [F_m^i(x)]' \cos(k_y^i y) \cos(k_z^i z), \\
H_z^i &= \sum_{m=0}^{+\infty} -\frac{k_y^i k_z^i}{(h^i)^2} C_m^i F_m^i(x) \sin(k_y^i y) \sin(k_z^i z),
\end{aligned} \tag{2}
$$

where C_m^i is the amplitude factor, k_z^i and k_y^i are the wave numbers in the z- and y-directions, respectively, $k_y^i = k_y^{\mathrm{I}} = l\pi/a$, $h^i = h^{\mathrm{I}}$, $k_z^i = m\pi/w$, $(m = 0, 1, 2\cdots)$. In region II, $F_m^{\mathrm{II}} = \cosh[\upsilon_m^{\mathrm{II}}(x-b-d)]$, and in region III, $F_m^{\mathrm{III}} = \cosh[\upsilon_m^{\mathrm{III}}(x+b+d)]$. $(F_m^i)'$ is their derivatives. Here $(\upsilon_m^i)^2 = (k_z^i)^2 - (h^i)^2$. Using the matching conditions of the fields at the boundaries between the regions, it is possible to obtain the dispersion relation, which determines the wave propagation.

2.2. Vacuum dispersion characteristics

The matching condition at $x = -b$ and $x = b$ is governed by the requirement for the continuity of the tangential component of the electric field on all interfaces (metallic and nonmetallic) as well as the continuity of the tangential component of the magnetic field on all nonmetallic interfaces, i.e. the following equations:

$$E_z^{\mathrm{I}}(b,y,z) = \begin{cases} E_z^{\mathrm{II}}(b,y,z), & 0 < z < w, \\ 0, & w < z < L, \end{cases} \tag{3}$$

$$H_y^{\mathrm{I}}(b,y,z) = H_y^{\mathrm{II}}(b,y,z), \quad 0 < z < w, \tag{4}$$

$$E_z^{\mathrm{I}}(-b,y,z) = \begin{cases} E_z^{\mathrm{III}}(-b,y,z), & 0 < z < w, \\ 0, & w < z < L, \end{cases} \tag{5}$$

$$H_z^{\mathrm{I}}(-b,y,z) = H_y^{\mathrm{III}}(-b,y,z), \quad 0 < z < w. \tag{6}$$

Substituting the components of the fields into the above-mentioned matching condition (3)–(6), the dispersion equation of the double rectangular waveguide grating SWS can be obtained. Due to the symmetrical characteristics of the structure, dispersion equation contains two kinds of modes: one is symmetrical mode and the other is anti-symmetric mode. Here, considering the completeness, both of the two modes are given. The uniform formula of the dispersion equation is written as

$$|X_{n,n'} - \delta_{n,n'} Y_n| = 0, \quad n, n' \in Z. \tag{7}$$

Here, for the symmetrical mode, we have

$$X_{n,n'} = -\frac{2}{w}\sinh(\upsilon_{n'}^{\mathrm{I}} b) \sum_{m=0}^{+\infty} \upsilon_m^i \tanh(\upsilon_m^i d) \frac{R(-\beta_{n'}^{\mathrm{I}}, k_z^i) R(\beta_n^{\mathrm{I}}, k_z^i)}{1+\delta_{m0}}, \tag{8}$$

$$Y_n = \upsilon_n^{\mathrm{I}} \cosh(\upsilon_n^{\mathrm{I}} b) L. \tag{9}$$

For the anti-symmetrical mode, we obtain

$$X_{n,n'} = -\frac{2}{w}\cosh(\upsilon_{n'}^{\mathrm{I}} b) \sum_{m=0}^{+\infty} \upsilon_m^i \tanh(\upsilon_m^i d) \frac{R(-\beta_{n'}^{\mathrm{I}}, k_z^i) R(\beta_n^{\mathrm{I}}, k_z^i)}{1+\delta_{m0}}, \tag{10}$$

$$Y_n = \upsilon_n^{\mathrm{I}} \sinh(\upsilon_n^{\mathrm{I}} b) L, \tag{11}$$

where δ_{m0} and $\delta_{n,n'}$ are Kronecker delta, and R is expressed as

$$R(\beta_n^{\mathrm{I}}, k_z^i) = \begin{cases} \mathrm{j}\beta_n^{\mathrm{I}} \dfrac{1 - \mathrm{e}^{\mathrm{j}\beta_n^{\mathrm{I}} w}(-1)^m}{(\beta_n^{\mathrm{I}})^2 - (k_z^i)^2}, & \beta_n^{\mathrm{I}} \neq \pm k_z^i, \\ \dfrac{w}{2}(1+\delta_{m0},), & \beta_n^{\mathrm{I}} = \pm k_z^i. \end{cases} \tag{12}$$

Generally speaking, the symmetrical mode, which is beneficial to the beam–wave interaction, has a longitudinal field much stronger than the anti-symmetrical mode, the longitudinal field of which is very weak in the central region. So, in the following discussion including the calculation of coupling impedance, we consider only the symmetrical mode. To simplify the calculation, only the lowest mode TE_{y10} is discussed, that is, $l = 1$. Figure 2 shows the dispersion characteristics of a double rectangular waveguide grating SWS. In order to check the calculated results, a three-dimensional electromagnetic simulation software CST is used for comparison. The smooth curve represents the theoretical results; the triangular points denote the results given by the CST simulation. It is obvious that the CST simulation data are in agreement with the theoretical results, which supports our theory.

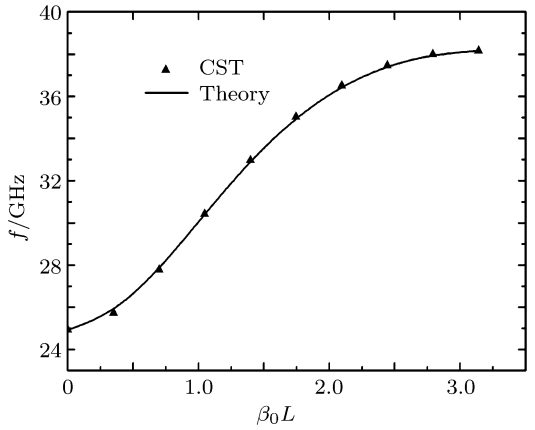


Fig.2. Dispersion curve for the double rectangular waveguide grating structure with dimensions in units of mm: $a = 6$, $b = 1$, $d = 2$, $w = 0.8$, $L = 1.6$.

As we know, for amplification in a travelling-wave tube, the electromagnetic wave and the beam must maintain synchronization with each other in a certain frequency (f) range, i.e. the z component of the phase velocity of the wave in the radio-frequency circuit must be close to the electron beam velocity. When the frequency varies, which makes the wave velocity differ from the electron velocity, the gain of the tube will decrease. Thus, the variation in the phase velocity with frequency is very important in the design of TWT and can determine its bandwidth. The phase velocity normalized by c in this structure is written as $v_\mathrm{p}/c = (k_0 a/\beta_0 L)(L/a)$.

Figure 3 shows the effect of variation in the groove-depth d on the normalized phase velocity-normalized frequency ($v_\mathrm{p}/c - k_0 a$) dispersion characteristic.

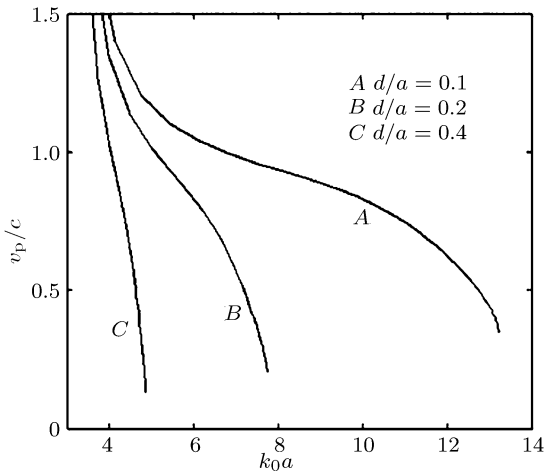


Fig.3. The dispersion curves for several values of the groove-depth d. Parameters in calculation: $b/a = 0.25$, $L/a = 0.08$, $w/L = 0.5$.

It is clear that, as the groove-depth d increases, forcing the wave to move towards the groove region, the phase velocity decreases and the dispersion curves become steeper. In addition, the influences of the variations in the grating-period and groove-width on the dispersion are shown in Figs.4 and 5 respectively. From

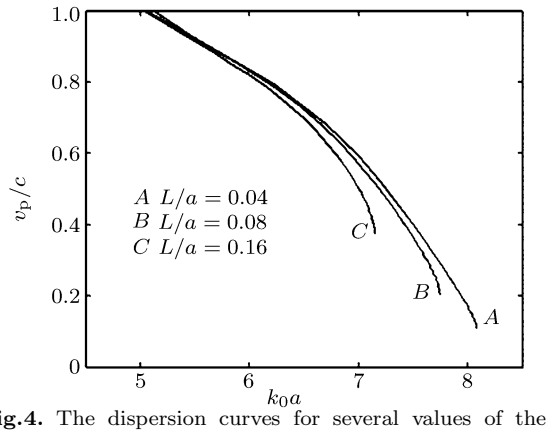


Fig.4. The dispersion curves for several values of the grating-period L. Parameters in calculation: $b/a = 0.25$, $d/a = 0.2$, $w/L = 0.5$.

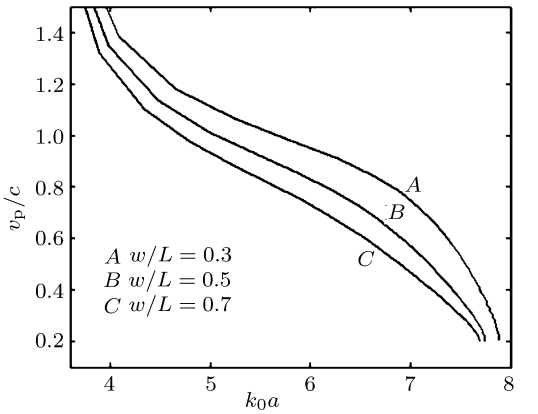


Fig.5. The dispersion curves for several values of the groove-width w. Parameters in calculation: $b/a = 0.25$, $d/a = 0.2$, $L/a = 0.08$.

Fig.4, we can see that the grating-period has no influence on dispersion except for the central frequency moving towards the lower frequencies as the grating-period increases. From Fig.5, it may be seen that the phase-velocity decreases and the bandwidth is basically unchanged as the groove-width increases.

2.3. Coupling impedance

For a slow-wave structure, whether it is useful or not depends on not only the dispersion but also the coupling impedance that represents the intensity of the interaction between the wave and the electron beam. From Pierce's theory,[12] the gain of the tube is proportional to the amplification parameter C, where $C^3 = K_{cn}/4V_0/I_0$, in which K_{cn} is the interaction impedance for the nth space harmonic wave and is defined as

$$K_{cn} = \frac{E_{zn}E_{zn}^*}{2\beta_n^2 P}, \tag{13}$$

where E_{zn} is the longitudinal component of the electric field of the nth space harmonic wave at the position of the electron beam, and E_{zn}^* is its conjugate component. We can obtain

$$E_{zn}E_{zn}^* = \left(\frac{\omega\mu_0 v_n^{\mathrm{I}}}{(h^{\mathrm{I}})^2}[A_n^{\mathrm{I}}\cosh(v_n^{\mathrm{I}}x) + B_n^{\mathrm{I}}\sinh(v_n^{\mathrm{I}}x)]\sin(k_y^{\mathrm{I}}y)\right)^2. \tag{14}$$

Define P as the total power flow along the z axis through the whole circuit system

$$P = \sum_{n=-\infty}^{+\infty} P_n^{\mathrm{I}} + \sum_{m=0}^{+\infty} P_m^{\mathrm{II}} + \sum_{m=0}^{+\infty} P_m^{\mathrm{III}}. \tag{15}$$

Here P_m^{II} and P_m^{III} are the power flows in regions II and III, but we note that both of them are zero because the group velocity of the grooves is zero. Then, P_n^{I} is the power flow of the nth space harmonic wave in region I, and can be written as

$$P_n^{\mathrm{I}} = \frac{1}{2}\mathrm{Re}\left(\int_0^a\int_{-b}^{b} E_x^{\mathrm{I}}(H_y^{\mathrm{I}})^*\mathrm{d}x\mathrm{d}y\right). \tag{16}$$

By using the dispersion equations, each component of the fields can be obtained. Substituting them into the expressions (13), (14) and (16), the coupling impedance of the nth space harmonic wave may be achieved. Assuming that the electron beam is present, and its width, thickness and position are δ, t, x_{e}, respectively. So the average coupling impedance is

$$\bar{K}_{cn} = \frac{1}{\delta\cdot t}\int_{(a-\delta)/2}^{(a+\delta)/2}\int_{x_{\mathrm{e}}}^{x_{\mathrm{e}}+t} K_{\mathrm{c}}(x,y)\mathrm{d}x\mathrm{d}y. \tag{17}$$

Using the results of the dispersion relations obtained in Section 2.2, we may calculate the coupling impedance according to the expression (13). Here, the coupling impedance is calculated by assuming that a sheet of electron beam passes through the surfaces of the grooves, i.e. the position of the electron beam is at $x = \pm b$. Note that all the quantities in the definition of the coupling impedance are 'cold' quantities: namely, they do not allow for the presence of the beam.

Figure 6 shows the coupling impedances of the fundamental wave (solid line) and –1 space harmonic wave (dashed line) as the groove-depth d changes. The

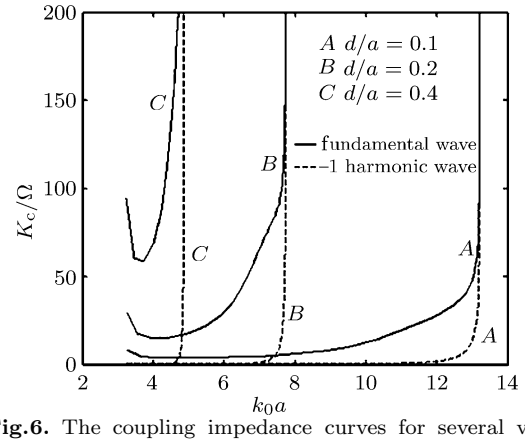


Fig.6. The coupling impedance curves for several values of the groove-depth d. Parameters in calculation: $b/a = 0.25$, $L/a = 0.08$, $w/L = 0.5$.

physical parameters are identical to those in Fig.3. Apparently, the coupling impedance increases with the increase of the groove-depth. This is because the z component of the electric field near the surface of the grating increases due to the increasing of the slot depth d. Thus, the structure with an appropriate groove-depth could achieve a larger coupling impedance. From Fig.6, the typical coupling impedance for the fundamental wave is much higher

than that for the –1 space harmonic wave, especially in a low frequency range, where its value is only about $0.05\,\Omega$. So the weak backward wave interaction may reduce the risk of the backward wave oscillating.

The effect of the grating-period on the coupling impedance of the fundamental wave is illustrated in Fig.7. It is shown that the coupling impedance K_c has a little change with the grating period. According to Fig.8, the coupling impedance increases as the groove-width increases and the bandwidth keeps unchanged.

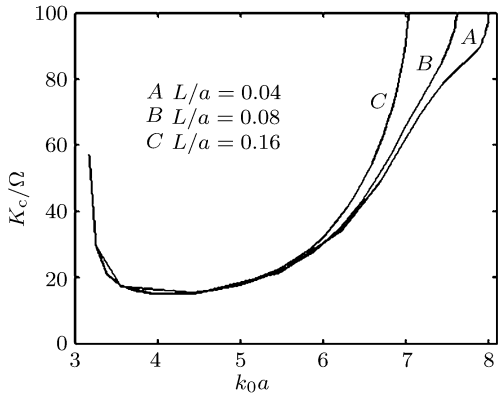


Fig.7. The coupling impedance curves for several values of the grating-period L. Parameters in calculation: $b/a = 0.25$, $d/a = 0.2$, $w/L = 0.5$.

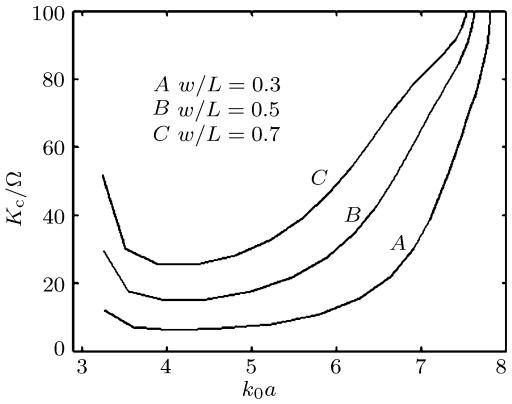


Fig.8. The coupling impedance curves for several values of the groove-width w. Parameters in calculation: $b/a = 0.25$, $d/a = 0.2$, $L/a = 0.08$.

3. Linear theory of a double rectangular waveguide grating TWT

In this section, we discuss the beam-wave interaction in the double rectangular waveguide grating TWT. We first derive the "hot" dispersion equation for this kind of TWT. The beam employed here is assumed to be a sheet electron beam under the influence of an infinite magnetic field B_0 in the z-direction; thus, it propagates uniformly along the z-axis of the system at a velocity v_0. This structure is shown in Fig.9. Because of the intervention of the electron beam, the structure is divided into five regions. Following the field-matching condition described in Section 2.2, the 'hot' dispersion equation can be derived by solving the equations of motion and continuity of the electron beam, and Maxwell's equations.

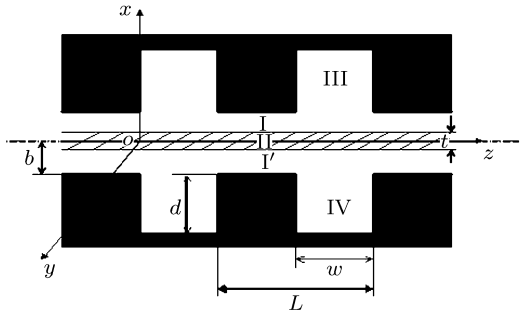


Fig.9. The double rectangular waveguide grating slow-wave structure with the electron beam.

The field expressions in regions I and I′ are the same as the expression (1), and the fields in regions III and IV are the same as the expression (2). The electron beam region is regarded as a sheet of travelling plasma. Because of the influence of the electron beam, the wave number v_{en}^{II} in the x-direction of region II is expressed as

$$v_{en}^{II} = \frac{(k_0^2\varepsilon_{en} - k_y^2)}{h^2}(v_n^I)^2. \tag{18}$$

Here $\varepsilon_{en} = 1 - \omega_p^2/(\omega - \beta_n v_0)^2$ is the relative dielectric constant, $\omega_p = \sqrt{\rho_0 e/\varepsilon_0 m_e}$ is the plasma frequency, $\rho_0 = J/v_0$ is the density of electric charge, $v_0 = \sqrt{2eV_b/m_e}$ is the speed of electron, J is the current density, e is the electron charge, ε_0 is the vacuum permittivity, m_e is the static electron mass, V_b is the accelerated velocity. In region II, the form of the field distribution is the same as in region I, the only difference is the wave number in the x-direction, expressed by v_{en}^{II}.

The field matching condition at $x = \pm b$ is the same as that obtained in Section 2.2. The boundary condition at the surface of the electron beam is given as follows:

$$E_z^I = E_z^{II}, \quad E_z^{I'} = E_z^{II}, \tag{19a}$$

$$H_y^I = H_y^{II}, \quad H_y^{I'} = H_y^{II}. \tag{19b}$$

Using the matching condition, the dispersion equation with electron beam can be written as

$$|X_{n,n'} - \delta_{n,n'} Y_n| = 0, \quad n, n' \in Z. \tag{20}$$

Here, only the symmetrical mode is of benefit to beam-wave interaction and should be taken into consideration. So we have

$$X_{n,n'} = -\frac{2}{s}[O_{n'} \sinh(\upsilon_{n'} b) + M_{n'} \cosh(\upsilon_{n'} b)] \sum_{m=0}^{+\infty} \upsilon_m \tanh(\upsilon_m d) \frac{R(-\beta_{n'}, k_m^i, w) R(\beta_{n'}, k_m^i, w)}{1 + \delta_{m0}}, \tag{21}$$

$$Y_n = \upsilon_n [O_n \cosh(\upsilon_n b) + M_n \sinh(\upsilon_n b)] L, \tag{22}$$

where

$$O_n = \frac{1}{h_{\rm en}^2 \upsilon_n} [h^2 \upsilon_{\rm en} \cosh(\upsilon_{\rm en} t) \cosh(\upsilon_n t) - h_{\rm en}^2 \upsilon_n \sinh(\upsilon_{\rm en} t) \sinh(\upsilon_n t)], \tag{23}$$

$$M_n = \frac{1}{h_{\rm en}^2 \upsilon_n} [h_{\rm en}^2 \upsilon_n \sinh(\upsilon_{\rm en} t) \sinh(\upsilon_n t) - h_n^2 \upsilon_{\rm en} \cosh(\upsilon_{\rm en} t) \cosh(\upsilon_n t)]. \tag{24}$$

The significances of the parameters in the expressions (20)–(24) are the same as those in Section 2.2. In the absence of the electron beam, the 'hot' dispersion (20) reduces to the expression (7). The complex transcendental equation for k_0 and β_0 in the expression (19) is solved using the downhill method.[13] Once the electron parameters and the dimensions are given, the relation between ω and β_0 can be established. The small signal gain per period of a double rectangular waveguide grating TWT can be given by

$$\begin{aligned} G(\text{dB/period}) &= 20 \log\{\exp[\text{Im}(\beta_0 L)]\} \\ &= 8.686 \text{Im}(\beta_0 L), \end{aligned} \tag{25}$$

where 'Im' denotes the imaginary part of a complex number.

Here, we give the results of the small-signal gain per period versus the frequency under assumed beam parameters. In order to illustrate the amplification of this structure, Fig.10 shows the small-signal gain per period versus the normalized frequency for the dimensions: $b/a = 0.25$, $d/a = 0.2$, $L/a = 0.08$, $w/L = 0.5$, $t/a = 0.05$, $V_0 = 400\,\text{kV}$, $I_0 = 5\,\text{A}$. It is shown that the narrow-band amplification can be achieved in this kind of structure and the typical small-signal gain per period is about 0.45 dB. Its bandwidth is very narrow and the 3-dB bandwidth of the device may be only 4%.

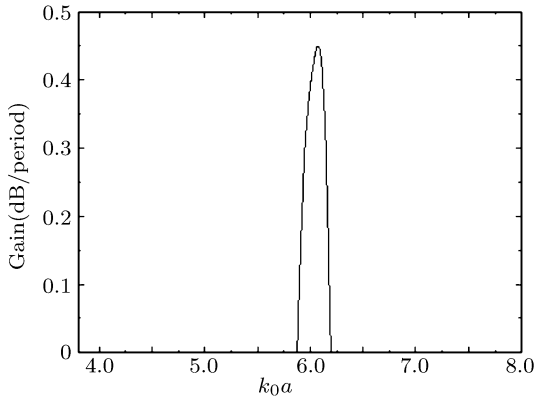


Fig.10. The small-signal gain versus the normalized frequency.

4. Conclusions

In this paper, a double rectangular waveguide grating SWS has been investigated for mm-wave TWT application. First, the wave properties of the structure in vacuum are analysed. The dispersion equation and the coupling impedance are derived and calculated numerically with the variation in physical dimensions. It is found that the structure has a very strong dispersion, and the coupling impedance for the fundamental wave is several tens of ohms, which will give rise to a relatively high gain in this structure. The coupling impedance of -1 harmonic wave is even less, therefore, the weak backward wave may reduce the risk of the backward wave oscillation. In addition, the numerical results agree well with those obtained from the CST microwave studio and support the theory.

The beam-wave interaction in this kind of TWT is examined. The 'hot' dispersion equation is derived and solved numerically by using the downhill method. The analysis reveals that this kind of structure is a narrow band amplifier.

References

[1] Carlsten B E 2002 *Phys. Plasmas* **9** 5088

[2] Maragos A A, Ioannidis Z C and Tigelis I G 2003 *IEEE Trans. Plasma Sci.* **3** 1075

[3] Zaginaylov G I, Hirata A, Ueda T and Shiozawa T 2000 *IEEE Trans. Plasma Sci.* **28** 614

[4] McVey B D, Basten M A, Booske J H, Joe J and Scharer J E 1994 *IEEE Trans. Microwave Theory. Tech.* **42** 995

[5] Joe J, Louis L J, Scharer J E, Booske J H and Basten M A 1997 *Phys. Plasmas* **4** 2707

[6] Louis L J, Scharer J E and Booske J H 1998 *Phys. Plasmas* **5** 2797

[7] Zhang J and Zhong H H 2005 *Acta Phys. Sin.* **54** 206 (in Chinese)

[8] Wei Y Y, Wang W X, Gong Y B and Zhou P 2000 *Acta Phys. Sin.* **49** 949 (in Chinese)

[9] Wei Y Y, Wang W X and Liu S G 2002 *Chin. Phys.* **11** 277

[10] Yue L N, Wang W X, Wei Y Y and Gong Y B 2005 *Acta Phys. Sin.* **54** 4223 (in Chinese)

[11] Wang G J, Gong Y B, Lu Z G, Wei Y Y and Wang W X 2005 *High Power Laser and Particle Beams* **17** 1137

[12] Pierce J R 1950 *Traveling Wave Tubes* (Princeton, NJ: Van Nostrand)

[13] Bach H 1969 *Commun. ACM* **12** 675